Validation of the Core Disruptive Accident constitutive law of the Castem-Plexus code on the Mara8 test

Marie-France Robbe, Jean-Yves Cariou, Michel Lepareux, Eloi Treille

Validation of the Core Disruptive Accident constitutive law of the Castem-Plexus code on the Mara8 test

M.F. Robbe[α], **Y. Cariou**[β], M. Lepareux[ξ], E. Treille[δ]

α CEA Saclay, DRN-DMT-SEMT, 91191 Gif sur Yvette cedex, France
Tel: (33) 1 69 08 87 49, Fax: (33) 1 69 08 52 42, E-mail: mfrobbe@cea.fr
β Novatome, NVPM, 10 rue Juliette Récamier, 69006 Lyon, France
ξ CEA Saclay, DRN-DMT-SEMT, 91191 Gif sur Yvette cedex, France
δ Socotec Industrie, 1 av. du Parc, 78180 Montigny le Bretonneux, France

Abstract

In case of a Hypothetical Core Disruptive Accident (HCDA) in a Liquid Metal Reactor, the interaction between fuel and liquid sodium creates a high pressure gas bubble in the core. The violent expansion of this bubble loads the vessel and the internal structures, whose deformation is important. The experimental test MARA8 simulates a HCDA in a mock-up closed by a flexible vessel and a flexible roof. This paper describes the MARA8 test-facility, the numerical simulation and its main results, and finally a comparison of the results computed by CASTEM-PLEXUS with the experimental results as well as other numerical results issued from previous simulations with the codes SIRIUS and CASTEM-PLEXUS.

Keywords

Core Disruptive Accident, nuclear reactor, explosion, fluid-structure coupling

1 Introduction

In case of a Hypothetical Core Disruptive Accident (HCDA) in a Liquid Metal Reactor, the interaction between fuel and liquid sodium creates a high pressure gas bubble in the core. The violent expansion of this bubble loads the vessel and the internal structures, whose deformation is important.

During the 70s and 80s, the LMFBR integrity was studied through several experimental programmes undertaken by several countries and by developing computer codes especially devoted to the analysis of transient loads resulting from a HCDA. The codes generally aimed at simulating a HCDA at reactor scale in order to demonstrate the capacity of the reactor to resist to such an accident. The experimental programmes had more varied objectives. For instance, the purpose of the FTR and CBR detail scale model [1] was to demonstrate that the Clinch River Breeder Reactor could withstand HCDA loads for licensing the reactor.

The STROVA and COVA programmes were dedicated to the validation of the computer codes. The STROVA programme [2] consisted in applying well defined transient loadings to a variety of metal structures (representative of the reactor roof and reactor vessel components)

and to compare the experimental results with those computed by the structural dynamics code EURDYN.

The COVA programme (COde VAlidation) [3] [4] [5] relied on a series of experiments performed in cylindrical tanks, starting with simple tests and increasing in complexity in such a way that only one new feature was introduced at a time. This programme aimed at validating [6] [7] the codes ASTARTE and SEURBNUK.

The WINCON and MARA programmes involved tests of gradual complexity which were based on a small scale replicas of real reactors. The interest of the WINCON programme (WINfrith CONtainment) [8] was at once to understand the influence of the presence of every internal structure in the global response of the reactor and to validate the codes SEUBNUK and EURDYN.

Based on a 1/30 scale model of the Superphenix reactor, the French programme MARA involved ten tests of gradual complexity due to the addition of internal deformable structures:
- MARA 1 and 2 considered a vessel partially filled with water and closed by a rigid roof [9],
- MARA 4 represented the main core support structures [10],
- MARA 8 and 9 were closed by a flexible roof [11],
- MARA 10 included the core support structures and a simplified representation of the above core structure (ACS) [12].

The SIRIUS french code [13] [14] was validated on the MARA programme [15] [16]. As other codes using a Lagrangian approach, SIRIUS needed rezonings during calculation because the internal structure presence caused high distortion of the fluid meshes. Finite differences were used for the sodium and the roof and finite elements for the thin vessel. As the argon and the bubble were not meshed, a law related volume to pressure.

At the end of the 80s, it was preferred to add a specific HCDA sodium-bubble-argon tri-component constitutive law [17] to the general ALE fast dynamics finite element CASTEM-PLEXUS code. The HCDA constitutive law was qualified [18] on the CONT benchmark [19].

In order to demonstrate the CASTEM-PLEXUS capability to predict the behaviour of real reactors [20] [21], axisymmetric computations of the MARA series were confronted with the experimental results. The computations performed at the beginning of the 90s showed a rather good agreement between the experimental and computed results for the MARA 8 and MARA 10 tests even if there were some discrepancies which might be eliminated by increasing the fineness of the mesh [22].

As the method used for dealing with the fluid-structure coupling was improved since then, it was undertaken another comparison between the experimental and numerical results and a more detailed analysis of the results. The numerical results were already presented in [23]. After a brief presentation of the MARA8 test-facility, this paper is focused on the numerical model, the description of the main results and the comparison with the experimental results and previous numerical ones.

2 Description of the MARA8 test-facility

The MARA8 experiment belongs to the MARA test programme defined and realised at the CEA-Cadarache in order to simulate a HCDA in small scale (1/30) mock-ups of the Superphenix reactor block. The external dimensions of the MARA8 test were 55 cm of height and 35 cm of radius.

The characteristics of the mock-up were [22]:
- a scale factor of 1/30 for all dimensions and thickness,
- an axisymmetric geometry,
- sodium was represented by water, argon by air and the bubble expansion by an explosive source.

All tests of the MARA series were fired using a 45 g low density low pressure explosive charge of L54/16 composition [24] leading at least to a 1000 MJ full scale energy release [15]. The bare vessels were filled with water leaving a 4.3 cm air gap [11]. All the vessels were identical and made of 316 steel of 1.2 mm thickness, except between the junctions with the core support plate and the internal heat exchangers where the thickness was locally reduced from 0.9 to 1.1 mm in order to simulate a pinned attachment with the diagrid.

In MARA8, a flexible roof of 10 mm thickness A42 steel was clamped to the roof support [11]. The vessel was welded to a flange bolted to the roof support. The MARA8 test-facility (Fig. 1) did not include internal structures. The explosive charge was hung from the roof centre.

The whole test was well instrumented with:
- 7 pressure transducers fitted under the roof at different radii,
- 8 strain gauges placed on the upper and lower sides of the roof at three radial locations (centre, mid-radius and near the boundary),
- 6 strain gauges attached at three main locations on the vessel (upper bulge, charge level and base) to obtain axial and hoop strains,
- 2 high speed cameras used to obtain displacements of the roof and the vessel (upper bulge and base),
- residual deformations were evaluated by measuring, before and after the firing, mesh sizes of the grid drawn on the vessel and the roof.

3 Numerical modeling of the test-facility

The MARA8 test-facility is composed of structures and fluids interacting with each other. The mock-up is surrounded by a flexible roof and a flexible vessel. The structures are assumed to be thin and flexible enough to be represented by shells.

In case of a HCDA, the internal fluids are sodium, argon and a gas bubble. In the test, these fluids were respectively replaced by water, air and an explosive charge. Water and air were initially at the atmospheric pressure whereas the explosive charge induced an initial pressure of 165 MPa in the bubble area. The CDA model of the CASTEM-PLEXUS code is described in [23]. The characteristics taken into the numerical model are:

• Water	: $\rho = 998.3$ kg/m3	sound speed $C = 1550$ m/s	$p^{(0)} = 10^5$ Pa
• Air	: $\rho = 1.206$ kg/m3	$\lambda = c_p/c_v = 1.4$	$p^{(0)} = 10^5$ Pa
• Explosive charge	: $\rho = 400$ kg/m3	polytropic coef. $\eta = \lambda = 1.24$	$p^{(0)} = 1.646\,10^8$ Pa

Two kinds of fluid-structure coupling are available in the CASTEM-PLEXUS code. Their main differences lie in the definition of the local normal vector used to write the coupling relations between the freedom degrees of the fluid and the solid. The first fluid-structure coupling (FS2D instruction) requires the definition of coupling elements by the user and imposes to the fluid nodes to have the same displacements as the structure nodes. Besides, there is no automatic actualisation of the ALE grid for the elements other than the ones on the coupled lines. The second coupling (FSA instruction) goes without coupling elements; the code considers directly the fluid and solid nodes in contact and writes relations allowing a possible tangential movement of the fluid in relation to the structure. The FSA coupling is well adapted to complex geometries but it often implies a user intervention to pilot the displacements of the fluid ALE grid.

For the MARA8 test, the FS2D coupling was adopted because the geometry was sufficiently simple to define coupling elements easily and no huge distortion of the fluid mesh was waited. Owing to the symmetry of the mock-up, an axisymmetric representation (Fig. 2) was used for the numerical simulation.

The boundary conditions are:
- No horizontal displacement on the symmetry axis,
- No rotation of the two vessel and roof nodes located on the symmetry axis,

• Complete blocking of the node in the top corner at the junction between the vessel and the roof.

4 Analysis of the results computed with CASTEM-PLEXUS

In this part, we try to present a synthesis of the results computed with the current CASTEM-PLEXUS model. We use the whole information contained in the complete set of drawings.

Initially, a high pressure is concentrated in the central bubble and the fluids are resting. Since the beginning of the computation, the gas contained in the bubble starts expanding and a pressure wave propagates spherically.

The pressure wave impacts the vessel bottom at 0.14 ms. The water and the bubble are expelled from the central part of the mock-up. The impact of the pressure wave against the vessel bottom causes a local downward movement of the vessel since that time.

From 0.14 ms to 0.22 ms, the pressure wave moves laterally and impacts the lower part of the lateral wall of the vessel. The fluid impacts all the vessel bottom and the lower mid-height of the lateral wall. The lateral wall begins moving radially from 0.2 ms, thus initiating the formation of a lower bulge. We note the presence of stresses in the vessel bottom but the displacement remains elastic.

Between 0.22 ms and 0.5 ms, the pressure wave is pushed back by the lateral wall towards the top centre of the mock-up. The fluid speeds are oriented diagonally. The size of the gaseous central zone reaches now one third of the vessel radius.

The air layer located near the symmetry axis is compressed by the liquid water against the roof. Water arrives in the initial air zone with upwards velocities, overall in the vicinity of the roof centre. The pressure increases slightly under the roof. We observe simultaneously the creation of the lower bulge and the deformation of the vessel bottom. The vessel in submitted to stresses at the bottom and in the bottom corner.

From 0.5 to 1.5 ms, the gaseous central zone continues expanding with a spherical shape. The water in the lower part of the mock-up continues to move towards the vessel bottom and to impact it. We also notice untidy water movements near the bottom corner. Progressively, the fluid near the lateral wall orients upwards. These fluid movements cause a stress increase in the vessel bottom and the lateral wall and the appearance of plastic strains at the bottom, in the bottom corner and in the lateral wall. The lower bulge formation and the bottom subsidence are continuing.

In the same time, we note a massive arrival of water towards the roof and an horizontal outwards directed movement of air towards the top corner. The air layer is compressed below the roof and pushed outwards.

Between 1.5 and 3.5 ms, the water along the lateral wall goes up vertically. A circular fluid movement globally upward directed constitutes around the bubble. Under the roof, the water impacts the roof vertically. Air is concentrated in the top corner and the air zone has a minimum size at 3 ms.

The vessel bottom and the lower bulge go on deforming. The plastic strains increase at the bottom and stay constant at the lower bulge level. Under the water thrust, the roof suffers a first pressure peak and an upward deformation starting at the centre and progressing laterally. The stresses increase at the roof centre. Owing to the concentration of air in the top corner and the massive arrival of water upward directed along the lateral wall, an upper bulge starts creating near the top corner.

Between 4 and 5 ms, the central gaseous zone reaches the mock-up bottom but a liquid layer still exists along the vessel bottom. In the top corner, water impacts the vessel perpendicularly what causes the formation of the upper bulge and of a plastic hinge at the junction between the roof and the vessel. The stresses increase at the level of the upper bulge, as well as plastic strains appear.

There is a general upward water and bubble gas movement in the whole mock-up, except in the top corner. This massive water movement has for consequence the formation of a second pressure peak under the roof and a general deformation of the roof. In parallel, the air bag in the top corner is evicted along the walls: horizontally along the roof and downwards along the vessel.

Later, we note a progressive decrease of the water speeds and a relaxation of the air in the corner. Consequently the air zone becomes bigger. Because of the pressure decrease in the lower part of the vessel, the vessel bottom slightly goes back upwards.

5 Comparison of the experimental results and the numerical results

The purpose of our computations consisted in validating the HCDA constitutive law of the CASTEM-PLEXUS code and to estimate the progress realised in the modeling of the accident. Thus the current numerical results were compared with the experimental results and previous numerical results computed with the codes SIRIUS [11] and CASTEM-PLEXUS [22].

The comparison concerns:
- the vertical displacement of the vessel bottom and the instant of the maximum,
- the hoop strain, the instant of maximum and the distance to the roof of the vessel upper bulge,
- the hoop strain and the instant of maximum of the lower bulge of the vessel,
- the vertical displacement and the instant of maximum of the roof,
- the impact pressure and the instant of maximum on the roof.

The figures 3 and 4 present the vertical displacements of the vessel bottom (on the symmetry axis) and of the roof (at the centre and at mid-radius) for the current CASTEM-PLEXUS computations. The figures 5 and 6 show the maximum radial displacements for the upper bulge and lower bulge of the vessel for the current computations.

The figures 7, 8 and 9 display respectively the pressure for the current CASTEM-PLEXUS computations, for the MARA8 experiment and the one obtained in the previous CASTEM-PLEXUS calculations. The results are collected in the table 1. The CASTEM-PLEXUS computations are noted CP in that table.

The SIRIUS results used for the comparison correspond to computations based on dynamic strain-stress curves [11]. The main differences between the old and new CASTEM-PLEXUS computations come from the mesh fineness and improvements in the treatment of the fluid-structure coupling. The figure 10 presents the mesh used in the previous CASTEM-PLEXUS calculations.

The results in the table 1 show that, concerning the vessel bottom, the new CASTEM-PLEXUS results (14 % error for the maximum vertical displacement) are in a better agreement than the old CASTEM-PLEXUS ones (18 % error) for the displacement and the time, but not so good as the SIRIUS ones (2 % error).

Regarding the hoop strains of the upper bulge, the new results (24 % error on the maximum hoop strain) are less precise than the CASTEM-PLEXUS old ones (11 % error), but results are more precise than the SIRIUS ones (30 % error). The instant of the larger upper bulge is a bit late for both CASTEM-PLEXUS calculations (5.3 and 5.5 ms instead of 5.0 ms in the test) while the time computed by SIRIUS is correct (5.1 ms). Concerning the distance between

the upper bulge and the roof, the new CASTEM-PLEXUS model improves a little the precision (6.7 cm in the new computations instead of 7.3 cm in the old ones, to compare to 4.8 cm in the experimental device) but SIRIUS finds almost the right value (5.0 cm).

As far as the lower bulge is concerned, the new results (4 % error) are better than the old CASTEM-PLEXUS ones (6 % error), themselves much better than the SIRIUS ones (18 % error) for the maximum strain.

For the roof displacements, the new results (10 % error for both maximum displacements at the centre and at mid-radius) are in a better agreement for the maximum displacement than the old CASTEM-PLEXUS ones (20 % average error) but the best ones were calculated by SIRIUS (5 % error). The displacement at the end of the old CASTEM-PLEXUS computations was better than the recent results. This difference might be lessen if the computation was continued for a longer time. The three codes find the exact time for the maximum displacement.

Regarding the pressure under the roof, the two experimental peaks are found by the code CASTEM-PLEXUS. The instant of the maximum of each peak fits perfectly but the peak amplitude is not correct. The computed first peak is much lower and much larger than the experimental one (from 4 MPa in the centre to 7 MPa at the edge, instead of 18 MPa in the test). On the contrary, for the second peak, the computation shows a high and thin peak in the centre (maximum value 40 MPa) and larger peaks elsewhere (maximum values 5 MPa) whereas the test presents a succession of small peaks.

One can remark that the second peak at the centre of the roof has a very different shape from elsewhere under the roof. Indeed, at one quarter of the radius and at mid-radius, the computed second peak presents a good similarity with the experimental values.

The amplitude of the computed second peak at the roof centre is a consequence of the high vertical speeds observed for the fluid on the symmetry axis. This behaviour difference between the centre of the model and the rest of the model may come from either a problem of boundary condition, or the use of an axisymmetric representation whose precision is known to be very bad near the mesh centre.

Nevertheless, the impulse on the roof seems to be correct because the computer code finds the right roof displacement. In addition, Cariou indicated in [22] that the pressure measurement in the test facility lacked precision what can partially explain the differences between the computed and experimental results. As the pressure computed with SIRIUS is not available in [11], there is no possibility to see if the same problems were observed with the SIRIUS code.

Globally, the new CASTEM-PLEXUS computations are in a better agreement with the experimental results than the previous CASTEM-PLEXUS ones. The comparison with the SIRIUS results show that, in some cases, the CASTEM-PLEXUS results are better than the SIRIUS ones and in other cases the SIRIUS results fit better with the experimental ones. Generally speaking, the three sets of numerical results are in a good agreement with the test.

6 Conclusion

In this paper, we presented a computation of the MARA8 test simulating a HCDA. The test consists in an explosion in a steel vessel covered by a flexible roof. An explosive charge is placed in the middle of the test-facility. The vessel is filled with water, topped by an air blanket below the roof. A specific HCDA constitutive law was developed in the CASTEM-PLEXUS code to simulate this kind of explosion.

The code computed successfully the explosion during 7 ms of physical time. The computation shows the propagation of a pressure wave from the explosive zone towards the external vessel. A large gaseous zone creates in the middle of the mock-up. The pressure wave impacts first the vessel bottom and then the lateral wall. A large lower bulge creates in the lower part of the lateral wall.

Later, the water is pushed back by the vessel; it goes upwards and impacts the roof. The roof suffers a high pressure peak and moves away starting from the centre and going to the lateral wall. The air layer is concentrated in the top corner under the thrust of the upward directed water. A second bulge appears in the top part of lateral wall of the vessel.

A comparison was realised between the experimental results, the ones issued from the current CASTEM-PLEXUS computations and previous ones computed by the same code and by the SIRIUS code. They show that globally the results of the three computations were in a good agreement with the test results. Apart from the results concerning the pressure under the roof, the new results of the CASTEM-PLEXUS code fit better with the experimental results than the previous ones.

For the following tests of the MARA series (MARA10 and MARS tests), specific developments for testing the influence of the internal structures were realised in the CASTEM-PLEXUS code [25] [26] [27].

References

[1] Cagliostro, D.J., Florence, A.L., Abrahamson, G.R., 1979. Scale modeling in LMFBR safety, Nuclear Engineering and Design 55, 235-247.
[2] Kendall, K.C., Adnams, D.J., 1986. Experiments to validate structural dynamics code used in fast reactor safety assessment, Science and Technology of Fast Reactor Safety, Vol. 2, British Nuclear Energy Society, London, England.
[3] Hoskin, N.E., Lancefield, M.J., 1978. The COVA programme for the validation of computer codes for fast reactor containment studies, Nuclear Engineering and Design 46, 17-46.
[4] Holtbecker, H., 1977. Testing philosophy and simulation techniques, Nuclear Engineering and Design 42, 75-87.
[5] Albertini, C., et al. The JRC-COVA programme: Final Report. Commission of the European Communities, Report EUR 8705, 1983. Nuclear Science and Technology, 1984, pp. 1-182.
[6] Wenger, H.U., Smith, B.L., 1987. On the origin of the discrepancies between theory and experiment in the COVA series, Proc. 9th Int. Conf. on Structural Mechanics In Reactor Technology, Vol. E, Lausanne, Switzerland, pp. 339-344.
[7] Kendall, K.C., Benuzzi, A., 1980. The COVA programme: Validation of the fast reactor containment code SEURBNUK, Nuclear Engineering and Design 57, 79-105.
[8] Sidoli, J.E.A., Kendall, K.C. The WINCON programme - Validation of the fast reactor primary containment codes. Proc. INE Int. Conf. On Nuclear Containment, Cambridge, England, April 1987. Nuclear Containment Structures, D.G. Walton, Cambridge University Press, 1988.
[9] Acker, D., Benuzzi, A., Yerkess, A., Louvet, J., August 1981. MARA 01/02 - Experimental validation of the SEURBNUK and SIRIUS containment codes, Proc. 6th Int. Conf. on Structural Mechanics In Reactor Technology, Section E3/6, Paris, France.
[10] Smith, B.L., Fiche, C., Louvet, J., Zucchini, A., August 1985. A code comparison exercise based on the LMFBR containment experiment MARA-04. Proc. 8th Int. Conf. on Structural Mechanics In Reactor Technology, Section E4/7, Brussels, Belgium, pp. 151-157.
[11] Fiche, C., Louvet, J., Smith, B.L., Zucchini, A., August 1985. Theoretical experimental study of flexible roof effects in an HCDA's simulation, Proc. 8th Int. Conf. on Structural Integrity In Reactor Technology, Section E4/5, Brussels, Belgium, pp. 139-144.
[12] Louvet, J., Hamon, P., Smith, B.L., Zucchini, A., August 1987. MARA 10: an integral model experiment in support of LMFBR containment analysis, Proc. 9th Int. Conf. on Structural Mechanics In Reactor Integrity, Section E, Lausanne, Switzerland, pp. 331-337.
[13] Blanchet, Y., Obry, P., Louvet, J., August 1981. Treatment of fluid-structure interaction with the SIRIUS computer code, Proc. 6th Int. Conf. on Structural Mechanics In Reactor Technology, Section B8/8, Paris, France.
[14] Daneri, A., Toselli, G., Trombetti, T., Blanchet, Y., Louvet, J., Obry, P, August 1981. Influence of the representation models of the stress-strain law on the LMFBR structures in an

HCDA, Proc. 6th Int. Conf. on Structural Integrity In Reactor Technology, Section E4/4, Paris, France.
[15] Louvet., J., August 1989. Containment response to a core energy release. Main experimental and theorical issues - Future trends, Proc. 10th Int. Conf. on Structural Mechanics In Reactor Integrity, Vol. E, Anaheim, pp. 305-310.
[16] Bour, C., Spérandio, M., Louvet, J., Rieg, C., August 1989. LMFBR's core disruptive accident. Mechanical study of the reactor block, Proc. 10th Int. Conf. on Structural Mechanics In Reactor Technology, Vol. E, Anaheim, pp. 281-287.
[17] Lepareux, M., Bung, H., Combescure, A., Aguilar, J., August 1991. Analysis of a CDA in a LMFBR with a multiphasic and multicomponent behaviour law, Proc. 11th Int. Conf. on Structural Mechanics In Reactor Integrity, Section E13/1, Tokyo, Japan, pp. 371-376.
[18] Casadei, F., Daneri, A., Toselli, G., August 1989. Use of PLEXUS as a LMFBR primary containment code for the CONT benchmark problem, Proc. 10th Int. Conf. on Structural Mechanics In Reactor Technology, Section E13/1, Anaheim, pp. 299-304.
[19] Benuzzi, A., 1987. Comparison of different LMFBR primary containment codes applied to a benchmark problem, Nuclear Engineering and Design 100, 239-249.
[20] Lepareux, M., Bung, H., Combescure, A., Aguilar, J., Flobert, J.F., August 1993. Analysis of an HCDA in a fast reactor with a multiphase and multicomponent behavior law, Proc. 12th Int. Conf. on Structural Mechanics In Reactor Integrity, Section E7/2, Stuttgart, Germany, pp. 197-202.
[21] Cariou, Y., Pirus, J.P., Avallet, C., August 1997. LMR large accident analysis method, Proc. 14th Int. Conf. on Structural Mechanics In Reactor Technology, Section P3/7, Lyon, France, pp. 395-402.
[22] Cariou, Y., Spérandio, M., Lepareux, M., Christodoulou, K., August 1993. LMFBR's whole core accident. Validation of the PLEXUS code by comparison with MARA tests, Proc. 12th Int. Conf. on Structural Mechanics In Reactor Technology, Section E7/4, Stuttgart, Germany.
[23] Robbe, M.F., Cariou, Y., Lepareux, M., Treille, E., September 2000. Numerical simulation of a Hypothetical Core Disruptive Accident in the MARA8 test with the CASTEM-PLEXUS computer code, Proc. European Congress on Computational Methods in Applied Sciences and Engineering (ECCOMAS), Barcelona, Spain.
[24] David, F., 1978. Etude d'une composition explosive flegmatisée. Applications à la déformation d'une cuve, Proc. Symposium sur les hautes pressions dynamiques, Paris, France.
[25] Robbe, M.F., August 1999. A porosity method to model the internal structures of a reactor vessel, Proc. 15th Int. Conf. on Structural Mechanics In Reactor Technology, Vol. B, Seoul, Korea.
[26] Robbe, M.F., Bliard, F., April 1999. A porosity model to represent the influence of structures on a fluid flow. Application to a hypothetical core disruptive accident, Proc. 7th Int. Conf. On Nuclear Engineering, paper 7819, Tokyo, Japan.
[27] Robbe, M.F., Cariou, Y. , Treille, E., Lepareux, M., September 2000. Numerical interpretation of the MARA10 test simulating a Hypothetical Core Disruptive Accident in a mock-up schematizing a reactor, Proc. European Congress on Computational Methods in Applied Sciences and Engineering (ECCOMAS), Barcelona, Spain.

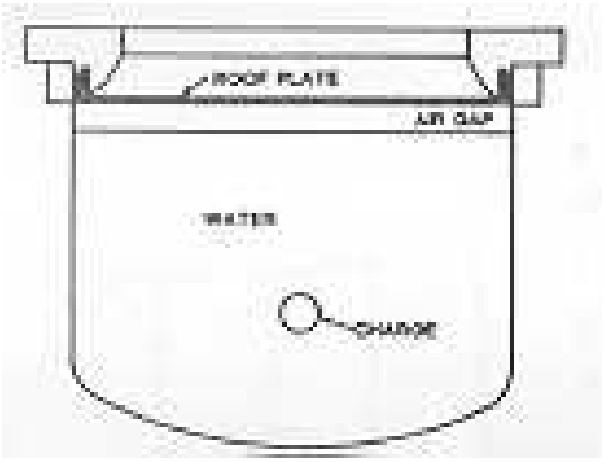

Fig. 1: The MARA8 test-facility

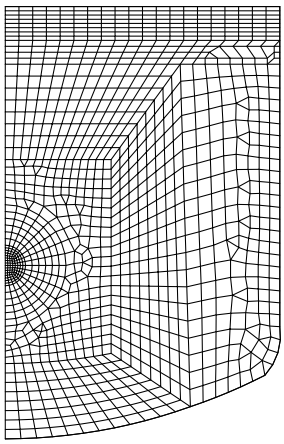

Fig. 2: Mesh of the MARA8 test

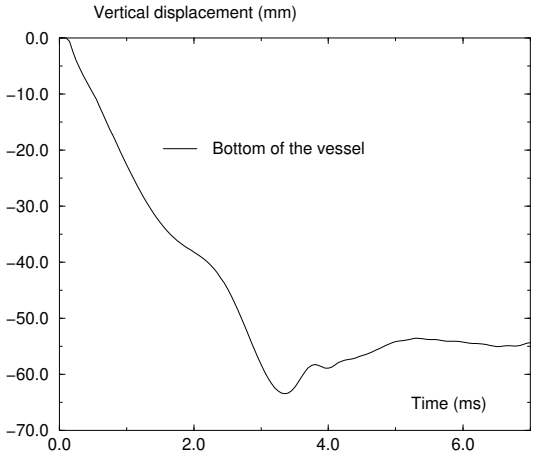

Fig. 3: Vertical displacement at the bottom of the vessel

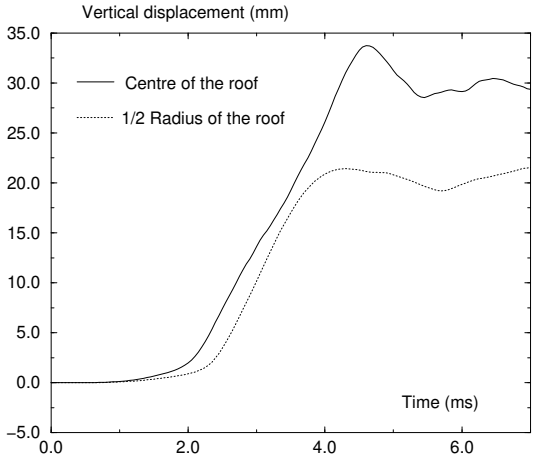

Fig. 4: Vertical displacement of the roof

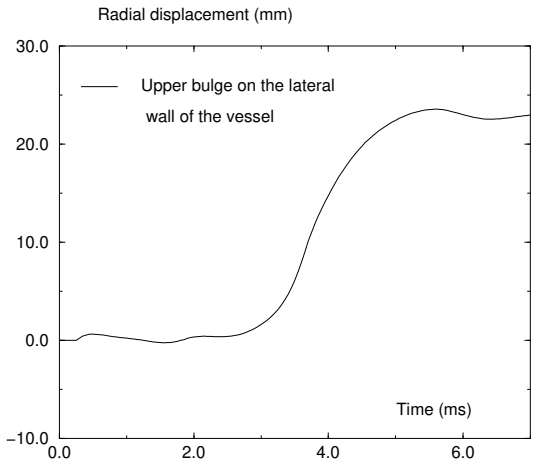

Fig. 5: Radial displacement on the upper bulge (lateral wall of the vessel)

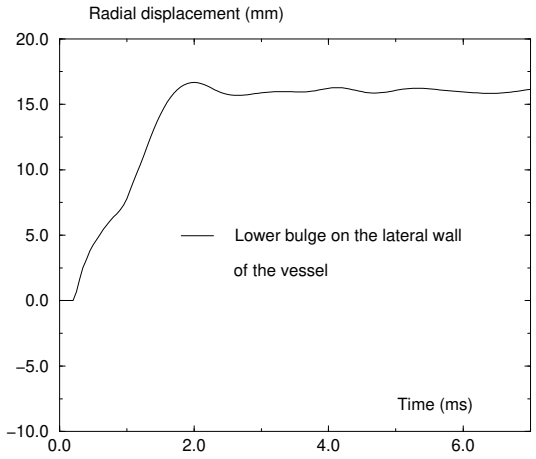

Fig. 6: Radial displacement on the lower bulge (lateral wall of the vessel)

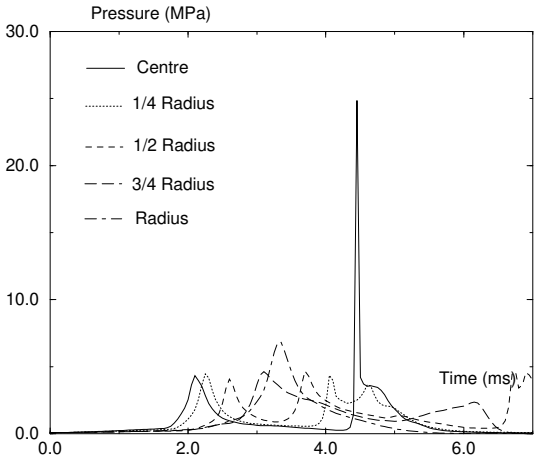

Fig. 7: Pressure under the roof

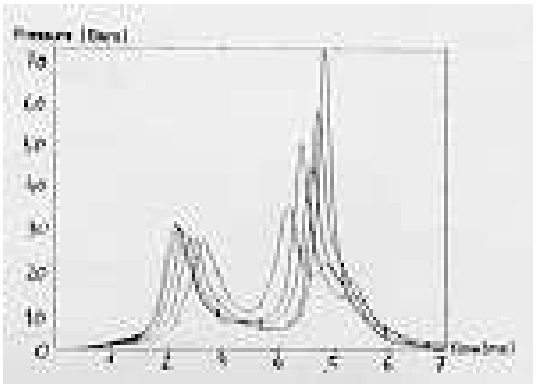

Fig. 9: Pressure under the roof, computed previously by CASTEM-PLEXUS

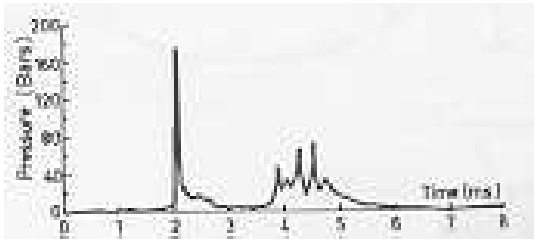

Fig. 8: Experimental pressure

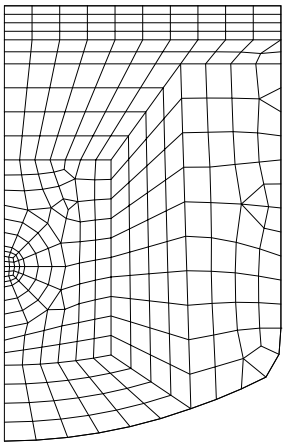

Fig. 10: Mesh of the previous CASTEM-PLEXUS calculations

		Experiment		SIRIUS computations		Old CP computations		New CP computations	
		Maximum	Final	Maximum	Final	Maximum	Final	Maximum	Final
Bottom of the vessel	Vert. displacement (cm)	5.5	5.2	5.4		6.5	5.7	6.3	5.4
	Instant of max (ms)	2.75		2.6		3.5		3.3	
Upper bulge of the vessel	Hoop strain (%)	5.4	4.6	3.8		6.0	5.5	6.7	6.5
	Instant of max (ms)	5.0		5.1		5.3		5.5	
	Distance to the roof (cm)		4.8		5.0		7.3		6.7
Lower bulge of the vessel	Hoop strain (%)	5.0	4.2	4.1		4.7	4.4	4.8	4.6
	Instant of max (ms)	1.7		1.7		2.0		2.0	
Roof	Vert. displacement at the centre (cm)	3.8	2.8	3.6		3.0	2.6	3.4	2.9
	Vert. displacement at mid-radius (cm)	2.4	1.9	2.3		2.0	1.8	2.2	2.2
	Instant of max (ms)	4.5		4.4		4.6		4.5	
Pressure under the roof		1^{st} impact	2^{nd} impact	1^{st} impact	2^{nd} impact	1^{st} impact	2^{nd} impact	1^{st} impact	2^{nd} impact
	Max. pressure (MPa)	18.0	7.2			3.0	8.0	centre: 4.0 else: 7.0	centre: 25. else:5.0
	Instant of max (ms)	2.1	4 to 5			2.2	4 to 5	2.1	3.5 to 6

Table 1: Comparison between the experimental results and the results computed bu SIRIUS and CASTEM-PLEXUS